A Variable-Temperature Diffuse Reflectance Infrared Fourier Transform Spectroscopy Study of the Binding of Water and Pyridine to the Surface of Acid-Activated Metakaolin

Carolina Belver,[†] Christopher Breen,[‡] Francis Clegg,[‡] Cesar E. Fernandes,[§] and Miguel A. Vicente*,[†]

Departamento de Química Inorgánica, Universidad de Salamanca, Plaza de la Merced, S/N. E-37008-Salamanca, Spain, Materials and Engineering Research Institute, Sheffield Hallam University, Sheffield S1 1WB, United Kingdom, and Núcleo de Investigação em Química Alimentar e Ambiental, Universidade da Madeira, Campus da Penteada, 9000-390 Funchal, Portugal

Received July 6, 2004. In Final Form: December 15, 2004

Four metakaolins were prepared by heating a Spanish kaolin at 600, 700, 800, and 900 °C for 10 h. Following preliminary optimization, these metakaolins were acid activated in 6 M hydrochloric acid at 90 °C for 6 h; the samples calcined at 600, 700, and 800 °C produced the highest surface area solids and were selected for further study. Variable-temperature diffuse reflectance infrared Fourier transform spectroscopy analysis of the resulting acid-activated metakaolins (AAMKs) identified a wide range of hydrogen bond strengths in adsorbed water at room temperature. Above 300 °C it was possible to fit the broad hydroxyl stretching band to seven contributing components at 3730, 3700, 3655, 3615, 3583, 3424, and 3325 cm^{-1}. As the sample temperature was increased, the 3730 cm^{-1} band increased in intensity as the water hydrogen bonded to AlOHAl was thermally desorbed. The other six bands decreased in intensity. The spectra of adsorbed pyridine indicated the presence of both Brönsted and Lewis acid sites on the surface of the air-dried AAMKs. Preheating the AAMK at 200 °C prior to pyridine sorption reduced the number of Brönsted acid sites and increased the number of thermally stable Lewis acid sites. A reduction in the amount of adsorbed pyridine after pretreating the AAMK at 400 °C was tentatively attributed to a reduction in surface area. This was reflected in fewer thermally stable Lewis acid sites in the AAMK pretreated at 400 °C compared to the number present in the sample pretreated at 200 °C.

1. Introduction

Acid activation is a chemical treatment that has been used for many years to improve the properties of clay minerals, particularly bentonites and montmorillonites. This treatment, which consists of leaching the clay with aqueous solutions of mineral acids, such as sulfuric, nitric, and, mainly, hydrochloric acid, produces acidic solids which have been used in industrial processes such as the cracking of oil, the decolorizing of oils, and the alkylation of phenols. The nature and properties of the resultant solids are largely determined by the treatment variables, such as acid concentration, acid-to-clay ratio, treatment temperature, time, and composition of the selected clay.[1−4]

The acid activation of a natural clay begins with the dissolution of the associated acid-soluble mineral impurities (calcite, dolomite, organic matter, etc.) and the replacement of the naturally occurring exchangeable cations on the clay by protons. Subsequently, the progressive removal of the cations from the octahedral sheet takes place, and if the treatment is sufficiently harsh, the structure of the tetrahedral sheet of the clay is drastically altered to form an amorphous silica gel phase, insoluble in acid media.[5] Consequently, the resulting acid-activated solids may be a mixture of unaltered clay layers and an amorphous silica phase, depending on the severity of the treatment. Usually, these solids exhibit considerably enhanced surface properties (specific surface area, surface acidity, porosity) compared to the pristine materials, and their use as catalysts,[3,6−10] as adsorbents or decoloring agents,[11−13] or in carbon-free copying paper[14] are among their most common uses.

Bentonites, which contain substantial quantities of montmorillonite, represent the most common natural clay minerals used for acid activation for both industrial uses and research investigations. The activation of other bentonitic (saponite-based clays) and fibrous (sepiolite or

* Corresponding author. Fax: +34-923-294574. E-mail address: mavicente@usal.es.
[†] Universidad de Salamanca.
[‡] Sheffield Hallam University.
[§] Universidade da Madeira.

(1) Mendioroz, S.; Pajares, J.; Benito, I.; Pesquera, C.; González, F.; Blanco, C. *Langmuir* **1987**, *3*, 676−681.
(2) Pesquera, C.; González, F.; Benito, I.; Blanco, C.; Mendioroz, S.; Pajares, J. A. *J. Mater. Chem*. **1992**, *2*, 907−911.
(3) Breen, C.; Zahoor, D. F.; Madejová, J.; Komadel, P. *J. Phys. Chem. B* **1997**, *101*, 5324−5331.
(4) Komadel, P. *Natural Microporous Materials in Environmental Technology*; NATO Science Series, Series E: Applied Sciences; Kluwer Academic Publishers: Dordrecht, 1998; p 3.
(5) Vicente, M. A.; Suárez, M.; Bañares, M. A.; López, J. D. *Spectrochim. Acta, Part A* **1996**, *52*, 1685−1694.
(6) Clark, J. H.; Cullen, S. R.; Barlow, S. J.; Bastok, T. W. *J. Chem. Soc., Perkin Trans*. **1994**, *2*, 1117−1130.
(7) Breen, C.; Watson, R.; Madejová, J.; Komadel, P.; Klapyta, Z. *Langmuir* **1997**, *13*, 6473−6479.
(8) Breen, C.; Moronta, A. *J. Phys. Chem. B* **1999**, *103*, 5675−5680.
(9) Komadel, P.; Janek, M.; Madejová, J.; Weekes, A.; Breen, C. *J. Chem. Soc., Faraday Trans*. **1997**, *93*, 4207−4210.
(10) Moronta, A.; Ferrer, V.; Quero, J.; Arteaga, G.; Choren, E. *Appl. Catal. A* **2002**, *230*, 127−135.
(11) Hymore, F. K. *Appl. Clay Sci*. **1996**, *10*, 379−385.
(12) Falaras, P.; Kovanis, I.; Lezou, F.; Seiragakis, G. *Clay Miner*. **1999**, *34*, 221−232.
(13) Falaras, P.; Lezou, F.; Seiragakis, G.; Petrakis, D. *Clays Clay Miner*. **2000**, *48*, 549−556.
(14) Fahn, R.; Fenderl, K. *Clay Miner*. **1983**, *18,* 447−458.

10.1021/la048323m CCC: $30.25
Published on Web 02/10/2005

palygorskite-based clays) materials has also been reported, yet despite the large natural abundance of kaolinitic materials, their acid activation has not been widely studied. This is mainly due to the high chemical inertness of these materials, particularly under acid conditions.[15] However, if the natural kaolinites are calcined at temperatures between 550 and 950 °C, this inertness toward acid attack is removed.[16] The new phases formed upon calcination, known as metakaolinites, are considerably more amorphous than kaolinite itself and ^{27}Al magic angle spinning (MAS) NMR has shown that they contain a large number of reactive tetra- and pentacoordinated Al units, which makes them much more susceptible to acid modification than the original material.[17−19]

Fourier transform infrared spectroscopy has been widely applied to the study of metal oxides and hydroxides, including clays, and is particularly well suited to investigate the nature of surface hydroxyls (4000−3000 cm^{-1})[20−22] and their interaction with selected bases to probe the type and quantity of acid sites available to reactant species. Indeed the interaction of pyridine with solid acids remains one of the most widely used methods to characterize the number of Brönsted and Lewis acid sites via diagnostic, temperature-resistant bands at 1540 and 1450 cm^{-1}, respectively.[23,24]

We have recently reported a systematic study of the effect of hydrochloric acid concentration and treatment time at selected temperatures on the acid activation of various metakaolins, obtained by calcination of a natural kaolin at temperatures between 600 and 900 °C.[25,26] In the present paper, we present the infrared spectroscopic results for the binding of water and/or pyridine to the surface hydroxyls and undercoordinated Al ions at the surface of some selected acid-activated metakaolins (AAMKs).

2. Experimental Section

2.1. Materials. Kaolin from the Navalacruz deposit (Zamora province, west of Spain) has been used in the present study. More data about the characterization of this material can be found elsewhere.[25,26] The natural solid is composed of very pure kaolinite, with small amounts of montmorillonite, mica, and quartz as impurities. Prior to acid activation the quartz was almost quantitatively removed by sedimentation in water. The mineralogical composition of the ≤2 μm fraction thus obtained was estimated to be 94% kaolinite, 3% montmorillonite, and 3% mica. This sample has a BET surface area of 18 $m^2\ g^{-1}$.

The ≤2 μm kaolinite was calcined in air at 600, 700, 800, and 900 °C, thus forming metakaolins. Calcination was carried out in a programmable furnace, at a heating rate (from room temperature to the calcination temperature) of 10 °C min^{-1}. The solids were kept at the calcination temperature for 10 h. Following preliminary optimization, the calcined solids were acid activated using 6 M hydrochloric acid solutions (180 mL for 6.0 g of metakaolin), at 90 °C under reflux conditions, for 6 h. The activated solids were separated by centrifugation, washed with distilled water until no chloride anions could be detected, and dried at 50 °C. The sample designations identify the treatment history of each sample; e.g., MK-600-6-90-6 indicates that metakaolin was prepared by heating the kaolin at 600 °C before immersing in 6 M hydrochloric acid at 90 °C for 6 h.

2.2. Techniques. A complete physicochemical characterization of the solids has been reported previously, and the techniques used (chemical Analysis, X-ray diffraction, thermal analyses, nitrogen adsorption, electron microscopy, among others) are described in detail there.[25,26] In the present paper, we report only some data on the physicochemical characterization of the solids to understand their properties, and thus only a very general description of these techniques is given.

Elemental analyses of the solids were carried out by Activation Laboratories Ltd., Ancaster, Ontario, Canada, using inductively coupled plasma spectroscopy (ICPS) and atomic absorption spectroscopy (AAS). X-ray powder diffraction patterns were obtained by using a Siemens D-500 diffractometer, at 40 kV and 30 mA (1200 W), using Cu Kα filtered radiation. Thermal analyses were performed on Perkin-Elmer analyzers, TGA7 and DTA7, for gravimetric and differential thermal analyses, respectively. Textural analyses were carried out from the corresponding nitrogen adsorption−desorption isotherms at 77 K, obtained from a static volumetric apparatus (Micromeritics ASAP 2010 adsorption analyzer). The concentration of Brönsted acid centers has been calculated from the amount of cyclohexylamine retained by the solids, determined thermogravimetrically.[23,24]

The variable-temperature diffuse reflectance infrared Fourier transform spectroscopy (VT-DRIFTS) spectra were performed using a Mattson Polaris FTIR spectrometer equipped with a Graseby Selector DRIFTS accessory combined with an environmental chamber with a temperature range from 25 to 500 °C. Evolved gases were continuously removed using nitrogen gas (20 $cm^3\ min^{-1}$). The samples (0.25 g) were prepared as a 2% mixture with KBr and placed in the cup positioned in the environmental chamber. The first spectrum was collected before purging at 25 °C then after purging for 15 min. The sample was then heated to 50 °C and allowed to equilibrate for 15 min before collecting the spectrum. This process was repeated to 200 °C at 25 °C increments and then to 500 °C at 50 °C increments. Background spectra, collected using KBr under the same conditions, were used to ratio against the respective sample spectra. In the investigation with pyridine, the samples were dried in air at 25 °C, or at 200 or 400 °C for 24 h prior to exposure to vapor phase pyridine for 48 h. The samples were transferred directly from the pyridine vapor to the environmental chamber, and the spectra were collected employing the conditions described above.

Spectral fitting was performed by GRAMS/AI software using Gaussian components in all cases. Before fitting analysis, the spectra were smoothed and a baseline correction was performed between 3800 and 3200 cm^{-1}.

3. Results and Discussion

3.1. Physicochemical Properties of the Solids. The complete physicochemical characterization of all the solids has been described elsewhere.[25,26] A short summary, with emphasis on the samples selected for the VT-DRIFTS study, is given here. The calcination of the parent kaolin at the four temperatures proved to be an effective way of producing metakaolins. The X-ray diffractograms of the metakaolins exhibited amorphous patterns, which no longer displayed the characteristic (001) peaks for the parent kaolinite and the montmorillonite impurity. The surface area decreased after calcination, to values of 9−11 $m^2\ g^{-1}$, which is about 50% of the value for the natural kaolin. The four metakaolins exhibited very similar properties, and no apparent differences between them could be deduced from routine characterization techniques.

The solids obtained after activation with 6 M hydrochloric acid under reflux conditions (90 °C) displayed the characteristic broad band of amorphous silica (between

(15) Lussier, R. J. *J. Catal*. **1991**, *129*, 225−237.
(16) Chandrasekhar, S.; Ramaswamy, S. *Appl. Clay Sci*. **2002**, *21*, 133−142.
(17) Lambert, J. F.; Millman, W. S.; Fripiat, J. J. *J. Am. Chem. Soc*. **1989**, *111*, 3517−3522.
(18) Okada, K.; Shimai, A.; Takei, T.; Hayashi, S.; Yasumori, A.; MacKenzie, K. J. D. *Microporous Mesoporous Mater*. **1998**, *21*, 289−296.
(19) Liu, Q.; Spears, D. A.; Liu, Q. *Appl. Clay Sci*. **2001**, *19*, 89−94.
(20) Farmer, V. C. *Clay Miner*. **1998**, *33*, 601−604.
(21) Farmer, V. C. *Spectrochim. Acta, Part A* **2000**, *56*, 927−930.
(22) Shoval, S.; Yariv, S.; Michaelian, K. H.; Lapides, I.; Boudeville, M.; Panczer, G. *J. Colloid Interface Sci*. **1999**, *212*, 523−529.
(23) Breen, C. *Clay Miner*. **1991**, *26*, 473−486.
(24) Breen, C. *Clay Miner*. **1991**, *26*, 487−496.
(25) Belver, C. Ph.D. Thesis in Chemistry, University of Salamanca (in Spanish), 2004.
(26) Belver, C.; Bañares, M. A.; Vicente, M. A. *Chem. Mater*. **2002**, *14*, 2033−2043.

Table 1. Chemical Composition of MK-600-6-90-6 Acid-Activated Metakaolin, Compared to That of the Natural Kaolin[a]

sample	SiO_2	Al_2O_3	Fe_2O_3	MgO	K_2O	TiO_2	CaO	Na_2O	H_2O	S_{BET}
natural kaolin	46.97	33.57	2.08	0.44	0.64	0.31	0.20	0.08	15.27	18
MK-600-6-90-6	75.98	6.70	0.30	0.29	1.17	0.74	0.06	0.05	14.25	219

[a] Specific BET surface areas ($m^2\ g^{-1}$) of both solids are also given.

20 and 40° 2θ), which first appeared in the diffraction traces and then increased in intensity as the leaching conditions became harsher. Chemical analysis data (Table 1) confirmed that this observation was accompanied by a partial, but substantial, dissolution of Al^{3+} cations, originally present in the octahedral sheet of the parent kaolin, together with a considerable increase in the weight percent of silica, reaching values up to 80% of the water-free contents.

The BET surface area of the activated solids strongly depends on the treatment conditions, reaching values of 219, 172, and 209 $m^2\ g^{-1}$ when the metakaolins obtained via calcination at 600, 700, and 800 °C, respectively, were acid activated under the same conditions (6 M HCl, 90 °C, 6 h).[25,26] The concentration of acid sites in these solids, derived from the thermogravimetric desorption of cyclohexylamine, were similar at 0.18 mmol g^{-1}. When longer acid treatment times (12, 18, and 24 h) were employed, the useful properties of the solids were considerably reduced. The BET surface area decreased to ≈22 $m^2\ g^{-1}$ and the concentration of acid centers to ≈0.12 mmol g^{-1}. This marked reduction in surface area has been observed when both layered smectitic and fibrous clay minerals are subjected to extensive leaching.[1,2] As the alumina-rich portions of the structure are removed, silica fronds are produced as the product of advanced leaching. These fronds collapse onto each other and retard the acid's access to the largely, unaltered core at the center of each clay particle.[1,2] The X-ray diffraction (XRD) patterns and X-ray fluorescence (XRF) data for the metakaolins, subjected to acid leaching herein, identified amorphous silica alumina as the component and no longer reported any discernible layer structure. Nonetheless, Okada et al.[27] have presented scanning electron micrographs which clearly show that the layered structure of the kaolin is maintained after calcination at 600 °C and subsequent acid leaching. Thus passivation by silica fronds can still occur during the acid leaching of metakaolin leading to a deterioration in the textural properties.

Upon acid treatment the water content increased from almost zero in the metakaolins to ≈25% in the activated products. This increase was attributed to the water adsorbed on the much increased surface of the activated solids. The acid-activated metakaolins derived from the samples calcined at 600, 700, and 800 °C were all similar, whereas the solids derived from leaching the metakaolin prepared at 900 °C were difficult to distinguish from the metakaolin itself. This behavior was attributed to the onset of sintering of the kaolinite particles during the 10 h soak at 900 °C. This is likely to be accompanied by the onset of the transformation of metakaolin to spinel and amorphous silica,[28] which has been observed at about 980 °C. Thus, the metakaolins obtained from calcination at 900 °C were very inert and were considered too unreactive to produce acid-activated solids with useful surface area and acidity.

With all these considerations, the acid-activated metakaolin obtained by refluxing the metakaolin, calcined at 600 °C, with 6 M hydrochloric acid at 90 °C for 6 h (designated MK-600-6-90-6) was chosen as a representative sample for a detailed VT-DRIFTS study encompassing both thermal dehydroxylation together with a study of the spectra obtained upon the adsorption of pyridine after pretreatment of the acid activated metakaolin at 25, 200, and 400 °C. The chemical composition and BET surface area of this solid, together with those for the natural kaolin, are given in Table 1. This solid consisted mainly of silica, and its high surface area reflects the substantial dissolution of the alumina component from the amorphous metakaolin in the absence of passivation by silica. Very small amounts of highly inert solids (feldspars, quartz) are also expected to be present, but the majority of the solid is considered to be silica−alumina domains in close proximity. The solids obtained from the metakaolins prepared at 700 and 800 °C (MK-700-6-90-6 and MK-800-6-90-6) were studied to a lesser extent for comparative purposes.

3.2. Infrared Analysis. 3.2.1. VT-DRIFTS Spectra for MK-600-6-90-6. Okada and co-workers[18] have studied similar samples leached with 20% sulfuric acid and have established, using ^{29}Si MAS NMR, that numerous $Si(OSi)_3OH$ groups are formed on the activated surface. This, together with their studies of the sorption of methanol and water on these leached samples,[29] established that the activation rendered solids with more hydrophilic surface than traditional fumed or pyrogenic silicas; the activation products have specific surface properties because they partly retained the structure of the initial silicic sheets. These investigators presented rudimentary transmission FTIR data for samples heated to elevated temperatures,[18] which were very similar to the spectra recorded here in Figure 1a. Before considering the spectra of the acid leached metakaolin samples in detail, it is valuable to recall that water in the vapor phase, which is not involved in hydrogen bonding, has an OH stretching band at 3755 cm^{-1}. In weakly hydrogen bonded water the OH stretching band occurs in the region 3590−3500 cm^{-1} and shifts to 3455 cm^{-1} in liquid water. The OH stretching band for strongly hydrogen bonded water appears below 3450 cm^{-1}.[30] The DRIFTS spectrum collected at 25 °C (Figure 1a, top spectrum) displayed a very broad OH stretching band with a maximum at 3360 cm^{-1} which extended from 2600 to 3800 cm^{-1}. This illustrated that there was a large number of adsorbed water molecules which experienced a wide range of hydrogen bond strengths as they interacted with the surface and each other. As the sample temperature was increased, the intensity and the width of this broad OH stretching band decreased indicating that the range of hydrogen bond strengths had been reduced and a new band near 3730 cm^{-1} emerged becoming very distinct at temperatures >300 °C. Davydov[31] and others[32] have reported a band at 3747 cm^{-1} which is assigned to isolated SiOH groups that are not involved in hydrogen bonding to either other SiOH

(27) Okada, K.; Shimai, A.; Kameshima, Y.; Yasumori, A. *Clay Sci*. **1998**, *10*, 259−290.
(28) Chen, C. Y.; Lan, G. S.; Tuan, W. H. *J. Eur. Ceram. Soc*. **2000**, *20*, 2519−2525.
(29) Okada, K.; Shimai, A.; Hayashi, S.; Yasumori, A. *Clay Sci*. **1999**, *11*, 73−82.
(30) Frost, R. L.; Van der Gaast, S. J. *Clay Miner*. **1997**, *32*, 471−484.
(31) Davydov, V. Ya. *Adsorption on Silica Surfaces*; Surfactant Science Series, Marcel Dekker Inc., New York, 2000; p 63.
(32) Zaki, M. I.; Hasan, M. A.; Al-Sageer, F. A.; Pasupulety, L. *Colloids Surf., A* **2001**, *190*, 261.

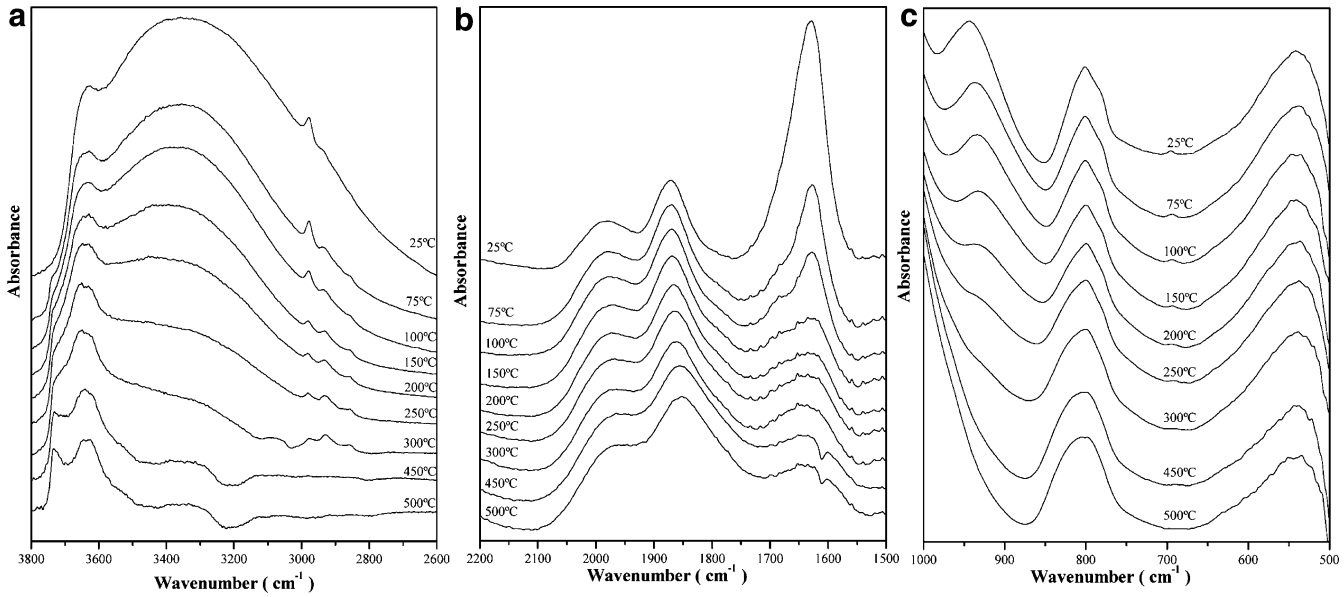

Figure 1. (a) VT-DRIFTS spectra for MK-600-6-90-6 in the OH stretching region (2600−3800 cm^{-1}) at the different temperatures indicated. (b) VT-DRIFTS spectra for MK-600-6-90-6 in the OH bending (1500−2200 cm^{-1}) at the different temperatures indicated. (c) VT-DRIFTS spectra for MK-600-6-90-6 in OH deformation region at the different temperatures indicated.

groups or water. Hence, they are often referred to as free SiOH groups. However, the band observed here was broader than that normally observed and downshifted by about 20 cm^{-1}, which could indicate the presence of SiOH groups involved in a small amount of H-bonding. However, it is more likely that this band should be assigned to a hydroxyl shared between two octahedrally coordinated aluminum ions since the band position was almost identical to the 3275 cm^{-1} position reported for alumina, silica−alumina,[32] and γ-Al_2O_3.[33] Note also that there was a significant shift in the baseline and the appearance of an artifact near 3220 cm^{-1} at 450 °C, due to baseline correction. Figure 1b shows that the intensity of the OH bending mode of adsorbed water at 1630 cm^{-1} had reduced to background levels by 200 °C. The bands at 1870 and 1985 cm^{-1} are combination bands similar to those reported for the $\nu_3 + \nu_4$ combination and $2\nu_2$ overtone bands for AlO(OH) in this region.[34]

The important change in the 500−1000 cm^{-1} region (Figure 1c) was the combined shift in position of the band at 935−920 cm^{-1} and the reduction in the intensity of this band, assigned to the OH bending mode of the $Si(OSi)_3OH$ groups.[18] There was very little residual intensity at 300 °C, but the band was not completely eradicated until 450 °C. These observations correlate with the loss of intensity under the stretching bands of hydrogen bonded OH (2600−3800 cm^{-1}) and may identify the loss of the surface hydroxyl groups upon which adsorbed water molecules cluster, i.e., as these $Si(OSi)_3OH$ groups diminished so did the water which was hydrogen bonded to them. Figure 2 illustrates how the total area under the broad OH stretching band (2500−3800 cm^{-1}) varied as the sample temperature was increased for all the samples studied. The general shape is the same although there are some minor differences in detail. Note the change of slope and the small plateau in the 150−200 °C region which correlated with a similar feature in the thermogravimetric weight loss curves for these samples and those reported by others.[18,27,35]

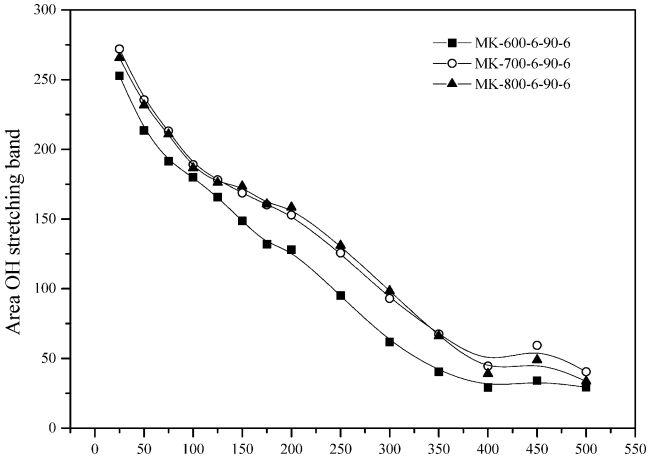

Figure 2. Temperature dependence of the total area under the OH stretching band (from 2500−3800 cm^{-1}) in the DRIFTS spectra for the different metakaolins indicated.

3.2.2. Peak Positions and Intensities Derived from Spectral Fitting. Below 300 °C it was impossible to fit an acceptable number of components to the broad OH stretching band (3200−3600 cm^{-1}), although the total band area could be determined (Figure 2). However, at $T \geq 300$ °C the fitting program consistently identified seven contributing bands which, in unconstrained fits, routinely converged on centers at 3731, 3699, 3655, 3615, 3538, 3424, and 3325 cm^{-1} (Table 2). Unequivocal assignment of the individual bands to a specific OH vibration was beyond the scope of this work, especially given the uncertainties associated with fitting such a broad spectral envelope and the minor shifts that would occur as sorbed water and surface OH groups were thermally desorbed. Nonetheless, comparison of these band centers with those for an appropriate selection of important comparators provided a useful insight into the nature of the OH groups in acid activated metakaolin and the groups available to interact with incoming molecules.

The first important observation was that there are no OH stretching bands above 3730 cm^{-1}. Others have reported terminal OH groups with stretching frequencies as high as 3792 cm^{-1} in Al_2O_3, at 3774 cm^{-1} in SiO_2/Al_2O_3,[32]

(33) Liu, X.; Pruett, R. E. *J. Am. Chem. Soc.* **1997**, *119*, 9856.
(34) Ram, S. *Infrared Phys. Technol.* **2001**, *42*, 547−560.
(35) Breen, C.; Taylor, S.; Burguin, E.; Centeno, M. *J. Colloid Interface Sci.* **2002**, *247*, 246−250.

Table 2. Spectral Fitting Data for the Hydroxyl Stretching Region of MK-600-6-90-6 in the Temperature Range 300−500 °C

nominal peak position/cm^{-1}	parameter	300 °C	350 °C	400 °C	450 °C	500 °C
3731	position/cm^{-1}	3730.97	3730.97	3730.97	3730.97	3730.97
	width/cm^{-1}	31.93	34.11	30.04	34.93	33.15
	area	1.86	2.23	2.41	2.57	2.49
3699	position/cm^{-1}	3698.81	3698.81	3698.81	3698.81	3698.81
	width/cm^{-1}	57.35	53.91	48.86	47.26	44.62
	area	5.43	4.91	4.14	3.21	2.46
3655	position/cm^{-1}	3655.33	3655.33	3655.33	3655.33	3655.33
	width/cm^{-1}	56.68	58.13	52.88	5719	55.74
	area	5.54	5.52	4.90	4.38	3.37
3615	position/cm^{-1}	3615.89	3615.89	3615.89	3615.89	3615.89
	width/cm^{-1}	72.24	75.95	70.98	76.42	73.76
	area	5.98	6.69	6.60	6.87	6.09
3538	position/cm^{-1}	3537.83	3537.83	3537.73	3537.83	3537.83
	width/cm^{-1}	153.33	146.85	121.12	105.16	90.53
	area	13.26	9.93	3.83	5.35	3.31
3424	position/cm^{-1}	3424.35	3424.35	3424.35	3424.35	3424.35
	width/cm^{-1}	108.63	104.32	73.60	98.40	106.91
	area	3.84	3.20	0.59	2.39	2.02
3325	position/cm^{-1}	3325.36	3325.36	3325.36	3325.36	3325.36
	width/cm^{-1}	145.70	124.31	118.63	121.59	103.89
	area	5.94	4.32	1.96	4.12	2.75

and 3764 cm^{-1} in γ-Al_2O_3.[33] Consequently, there were no appreciable quantities of either isolated, terminal AlOH or SiOH, which exhibits at band at 3745 cm^{-1},[30] groups in the AAMK structure. In contrast, the center of the fitted band at 3730 cm^{-1} correlates well with the presence of hydroxyl groups bridging between two octahedrally coordinated Al atoms, which are routinely observed in Al_2O_3, SiO_2/Al_2O_3, and γ-Al_2O_3.[32,33] The band at 3699 cm^{-1} was in excellent agreement with that observed at 3700 cm^{-1} in the spectrum of zeolite X heated at 400 °C,[36] while the fitted band at 3655 cm^{-1} agreed well with that observed for AlOH groups in zeolite X[36] and H−ZSM-5[37] at 3660 and 3662 cm^{-1}, respectively. The band near 3650 cm^{-1} in zeolites X and Y disappears upon exposure of the zeolite to pyridine vapor and is accompanied by the appearance of the diagnostic band for the pyridinium ion at 1540 cm^{-1}. The resulting zeolite/pyridine complex requires heating to temperatures in excess of 400 °C to restore the intensity of the OH stretching band at 3650 cm^{-1}, thus indicating that pyridine interacts very strongly with such an OH group in zeolites. It was interesting to note that the fitted band at 3615 cm^{-1} lay between the band positions reported for bridging SiOHAl in zeolite X (3625 cm^{-1}) and H-ZSM-5 (3609 cm^{-1}). However, given the uncertainty in the fitted band positions it is wise to exercise caution in accepting this interpretation given that there are AlOH bands near 3625 cm^{-1} in Al_2O_3[31] and at 3624 cm^{-1} in gibbsite, α-$Al(OH)_3$.[38] The fitted band at 3540 cm^{-1} can be confidently assigned to H-bonded OH groups given their presence in SiO_2, SiO_2/Al_2O_3,[31] and bayerite, α-$Al(OH)_3$.[38] Finally, the bands at 3424 and 3325 cm^{-1} were in reasonable agreement with those observed in bayerite, 3427 cm^{-1}, and boehmite, AlO(OH), 3310 cm^{-1},[34] respectively. Therefore, in summary acid activated metakaolin exhibited OH stretching bands that can be confidently assigned to AlOHAl groups such as those found in alumina, bayerite, gibbsite, and boehmite. These OH groups form hydrogen bonds with each other (3540 cm^{-1}) and most likely with adsorbed water. There was no clear evidence for a SiOH stretching frequency to accompany the $Si(OSi)_3OH$ band at 935 cm^{-1}. However, it was clear that the deformation mode of this OH group had been removed upon heating at 300 °C and the spectral fits were obtained at ≥300 °C. Finally, there was reasonable evidence for Brönsted acidity via the band near 3650 cm^{-1} and that for bridged AlOHSi groups (3625 cm^{-1}), which could be the origin of the

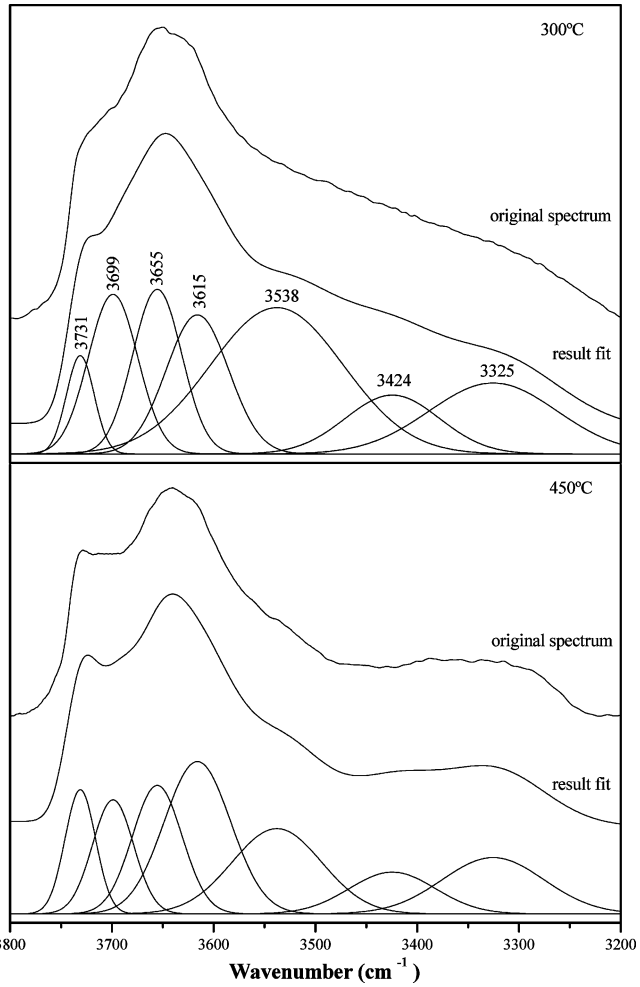

Figure 3. Representative fits of the spectra for MK-600-6-90-6 at 300 (upper) and 450 °C (lower).

(36) Guilleux, M. F.; Delafosse, D. *J. Chem. Soc., Faraday Trans. 1* **1975**, *71*, 1777.
(37) Buzzoni, R.; Bordiga, S.; Ricchiardi, G.; Lamberti, C.; Zecchina, A. *Langmuir* **1996**, *12*, 930−940.
(38) Lee, D. H.; Condrate, R. A. *Mater. Lett.* **1995**, *23*, 241−246.

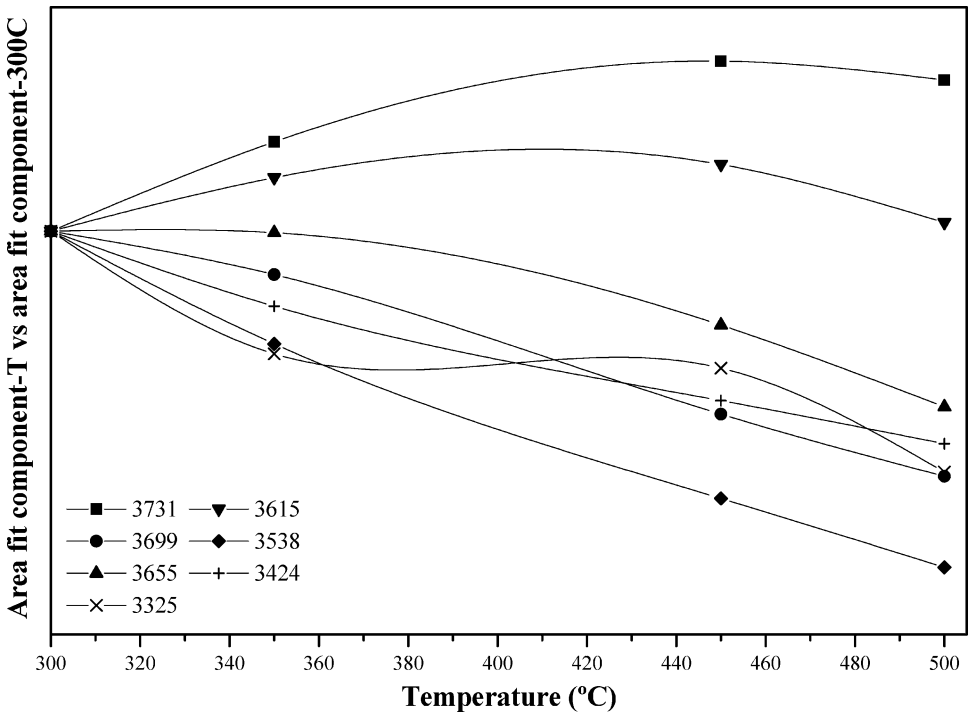

Figure 4. Temperature dependence of the area under the fitted components for MK-600-6-90-6, normalized to the fitted area of the individual bands at 300 °C.

diagnostic band for Brönsted-bound pyridine at 1545 cm^{-1} identified in the spectra of adsorbed pyridine (vide infra). It is generally accepted that pure alumina and pure silica do not exhibit any Brönsted acidity whereas the Brönsted acidity of silica−alumina increases with alumina content, maximizing at 50 wt % alumina and then diminishing to zero as the pure alumina is approached.[39] Thus, it appears that bridged AlOHSi groups occur at in MK-600-6-90-6 where silicon and aluminum share a common OH group. These are most likely to occur at the periphery of acid attack.

The peak positions of the individual components changed little as the sample temperature was raised, but the intensities under the components varied in a systematic manner. Representative fits of the spectra collected from sample MK-600-6-90-6 at 300 and 450 °C are shown in Figure 3, to illustrate the positions, intensities, and widths of the bands which emerged from the fitting program (Table 2). The most convenient way to illustrate the effect of temperature on the peak intensity was to normalize the areas under the contributing components to their area at 300 °C, and these data are presented in Figure 4. The 3731 cm^{-1} band increased with temperature whereas all the others, except for the peak at 3615 cm^{-1}, decreased with temperature. The increase in area of the 3615 cm^{-1} band probably occurred because the fitting program assigned too much intensity to the strong, broad 3538 cm^{-1} band at 300 °C (Figure 3, upper). Then, in subsequent fits this anomaly was rectified as the 3538 cm^{-1} band became weaker (as the number of OH groups decreased due to the loss of bound water and thermal dehydroxylation of the surface) and the program was able to more accurately divide intensity between the 3538 and 3615 cm^{-1} bands. The fluctuation in the area of the 3325 cm^{-1} band at 450 °C is attributed to the appearance of the artifact at 3220 cm^{-1}, which artificially enhanced the intensity of this band.

Overall, the fitting protocol reinforced the qualitative observations obtained from the raw data in Figure 1a. As the sample temperature was increased, the amount of hydrogen bonded OH decreased because water and/or hydroxyl groups were removed from the sample. Note also that the 3655 cm^{-1} band, which was tentatively assigned to AlOHSi, decreased in intensity while that for the AlOHAl (3730 cm^{-1}) increased. The increase in intensity of the 3730 cm^{-1} band was justifiably attributed to the removal of water hydrogen bonded to this bridging OH group. The area under the OH stretching band can be divided into two regions from 25 to 200 °C and from 200 to 400 °C (Figures 1a and 2); hence these were selected as the two sample pretreatment temperatures to be used prior to exposure to vapor phase pyridine. Moreover, 200 °C was the temperature at which the OH bending band (1630 cm^{-1}) reached background levels (Figure 1b) and 400 °C is almost identical to the temperature at which acid activated metakaolins samples were used to transform the gases evolved from pyrolyzed HDPE into useful, aromatic compounds.[35]

3.2.3. VT-DRIFTS Data for MK-600-6-90-6 after Exposure to Pyridine Vapor. Infrared spectroscopic investigation of pyridine-treated acidic solids can readily distinguish between Brönsted and Lewis acid sites on the surface and provide a semiquantitative estimation of the number of each type. Parry[40] and Ward[41] have assigned the bands for adsorbed pyridine, stating that bands at 1435 and 1445 cm^{-1} indicated the presence of physisorbed pyridine, that hydrogen bonded pyridine absorbs at 733, 1445, and 1590 cm^{-1} whereas Lewis bound pyridine exhibits bands at 1452, 1486, 1578, 1590, and 1606 cm^{-1}, and, finally, that Brönsted bound pyridine has an important diagnostic band at 1540 cm^{-1} together with bands at 1486 and 1635 cm^{-1}. With these assignments, the DRIFTS spectrum for pyridine saturated MK-600-6-90-6 at 25 °C (Figure 5a, bottom spectrum) exhibited bands

(39) Scokart, P. O.; Declerck, F. D.; Sempels, R. E. Rouxhet, P. G. *J. Chem. Soc., Faraday Trans. 1* **1977**, *73*, 359.

(40) Parry, E. P. *J. Catal*. **1963**, *2*, 317−379.
(41) Ward, J. W. *J. Colloid Interface Sci*. **1968**, *28*, 269.

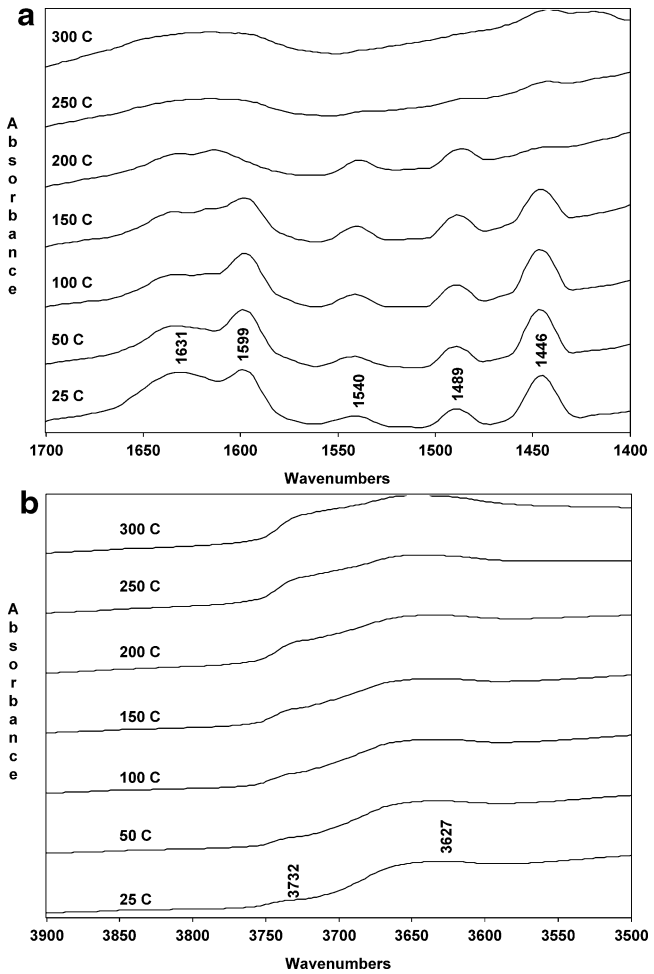

Figure 5. (a) VT-DRIFTS spectra in the 1400−1700 cm^{-1} region for air-dried MK-600-6-90-6 exposed to pyridine vapor. (b) VT-DRIFTS spectra in the 3500−3900 cm^{-1} region for air-dried MK-600-6-90-6 exposed to pyridine vapor.

due to Brönsted bound pyridine (BPYR) at 1631 and 1540 cm^{-1}. The 1446 cm^{-1} band, in combination with that at 1599 cm^{-1}, was assigned to hydrogen bonded pyridine, HPYR. The 1489 cm^{-1} band was attributed to contributions from BPYR and LPYR, although the Brönsted bound base is known to make a greater contribution to the intensity at this frequency. Raising the sample temperature to 150 °C reduced the intensity of the HPYR bands (1446 and 1599 cm^{-1}). At 200 °C the HPYR bands had been reduced to almost zero intensity and the remaining prominent bands were readily assigned to BPYR. At temperatures above 250 °C there was little evidence of any sorbed pyridine although there was a weak band near 1450 cm^{-1} which may suggest the presence of a small number of pyridine molecules bound to Lewis acid sites. The corresponding spectra in the OH stretching region (Figure 5b) revealed that as the hydrogen bonded pyridine was removed the AlOHAl groups at 3732 cm^{-1} became more distinct indicating that the portion of HPYR not bound to the pyridinium ions was bound to the surface AlOHAl groups. The reappearance of OH stretching bands, as hydrogen-bonded pyridine is desorbed, is a common observation in FTIR studies of pyridine-treated zeolites.[37]

Pretreating the MK-600-6-90-6 sample in nitrogen for 2 h at 200 °C prior to exposure to pyridine vapor resulted in distinct changes to the number, type, and thermal stability of sites that the adsorbed pyridine was bound to. The overall intensity of the spectrum collected at 20 °C (Figure 6, bottom spectrum) indicated that there was less

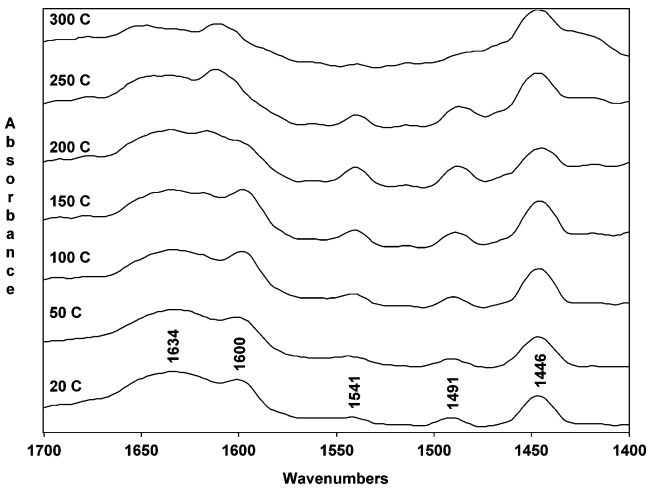

Figure 6. VT-DRIFTS spectra in the 1400−1700 cm^{-1} region for MK-600-6-90-6 heated at 200 °C for 2 h before exposure to pyridine vapor.

pyridine sorbed overall resulting in weak signals at 1541 and 1491 cm^{-1} (BPYR), although the HPYR bands at 1446 and 1600 cm^{-1} were still prominent. In the spectra collected between 50 and 150 °C, the BPYR band (1540 cm^{-1}) increased in intensity as the bands for HPYR became weaker. At 200 °C there was still clear evidence for pyridine adsorbed as HPYR and BPYR. This illustrates that HPYR was held to a higher temperature when the sample had been pretreated at 200 °C before exposure to pyridine compared with the unheated sample (Figure 5a). It is well established that pyridine molecules hydrogen bonded to the protonated BPYR molecules broadens, and reduces the intensity of the diagnostic BPYR band at 1540 cm^{-1} and that this band increases in intensity as the HPYR molecules are desorbed.[35,37] It was not possible to distinguish bands associated with pyridine hydrogen bonded to the free hydroxyl bands or to pyridinium ions, but it is anticipated that the pyridine will be thermally desorbed from the hydroxyl groups first. Hence the enhanced thermal stability of the HPYR in the sample pretreated to 200 °C was attributed to pyridine H-bonded to pyridinium ion. Note that a band at 1616 cm^{-1} had become more distinct as the temperature was raised from 150 to 200 °C and became a dominant band at 250 and 300 °C. In the same temperature interval the bands for BPYR at 1540 and 1490 cm^{-1} decreased in intensity and the 1600 cm^{-1} band was reduced to zero. It is important to realize that the band at 1446 cm^{-1} can be assigned to HPYR or LPYR and can only be distinguished by the greater thermal stability of the LPYR band. Thus, between 150 and 250 °C the signal from HPYR (1446 and 1600 cm^{-1}) was reduced to zero while the contribution from LPYR (1446 and 1616 cm^{-1}) became more evident. Thus after pretreating the sample in nitrogen at 200 °C for 2 h the number of Brönsted acid sites was decreased and the number of thermally stable Lewis acid sites was increased. Once again, the hydroxyl stretching region revealed that the 3728 cm^{-1} band of AlOHAl increased as HPYR was thermally desorbed (not illustrated).

The sample pretreated at 400 °C prior to exposure to pyridine vapor also exhibited significant differences in the detail of the spectra for adsorbed pyridine (Figure 7). The bands for HPYR were lost by 200 °C as in the unheated sample (Figure 5a) and once again the intensity of the BPYR band at 1540 cm^{-1} increased as the HPYR signal decreased reaching a maximum at 200 °C and then decreased as the BPYR was thermally desorbed. The intensity of the LPYR band at 1445 cm^{-1} was much weaker

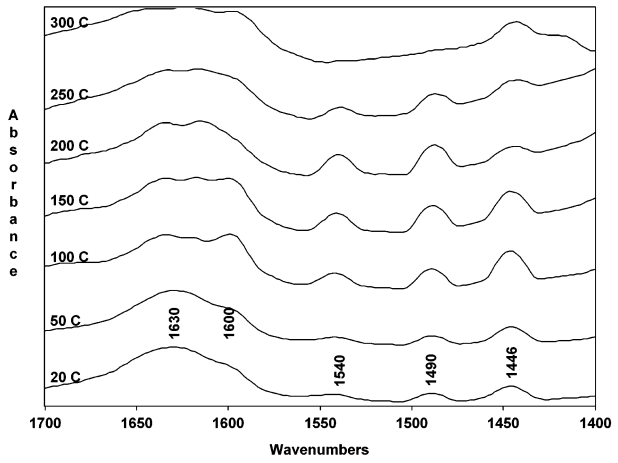

Figure 7. VT-DRIFTS spectra in the 1400−1700 cm^{-1} region for MK-600-6-90-6 heated at 400 °C for 2 h before exposure to pyridine vapor.

at temperatures >200 °C in comparison with the same band for the sample pretreated at 200 °C (Figure 6). At 300 °C only LPYR bands at 1445 and 1606 cm^{-1} were visible.

The conversion of Brönsted acid sites to Lewis acid sites is well established. In a classic study by Ward,[42] the IR spectrum of adsorbed pyridine was used to show that Brönsted acid sites were transformed into Lewis acid sites at pretreatment temperatures above 500 °C, when water formed from the decomposition of two adjacent Brönsted acid sites resulted in the formation of a Lewis site. Indeed pretreating MK-600-6-90-6 at 200 °C resulted in the most intense LPYR bands. This implies that 400 °C was too high a pretreatment temperature since it may have caused some partial collapse of the pore network, a possible loss of surface area, and/or a reduction in the accessibility of the acid sites to the pyridine probe.

4. Summary and Conclusions

The area under the broad hydroxyl stretching band of acid-activated metakaolin decreased as the sample temperature was increased, suggesting that water molecules experienced a wide range of hydrogen bond strengths when bound to the acid-activated metakaolin surface. As the temperature was increased, the range of hydrogen bond strengths and the number of water molecules bound to them decreased resulting in a weaker and narrower hydroxyl stretching band. Above 300 °C it was possible to fit this broad hydroxyl band to seven contributing components at 3731, 3699, 3655, 3615, 3583, 3424, and 3325 cm^{-1}. With the exception of the $Si(SiO)_3OH$ deformation band at 935 cm^{-1}, most of the other evidence, derived from the OH stretching region, indicated the presence of OH groups bound to Al or shared between Al and Si. As the temperature was raised, the 3731 cm^{-1} band increased in intensity and became better resolved due to the removal of water molecules hydrogen bonded to the AlOHAl groups which give rise to this band. All the other bands decreased in intensity as the water molecules and hydroxyl groups were thermally desorbed. No bands at higher frequencies than 3730 cm^{-1} were observed, confirming the absence of isolated terminal OH groups. There was reasonable evidence for AlOHSi groups at 3610 cm^{-1}, and the position of the 3650 cm^{-1} band was in close agreement with the more acidic site in zeolites X and Y. Of the remaining four bands near 3700, 3580, 3420, and 3320 cm^{-1}, a 3700 cm^{-1} band has been recorded in zeolite X heated to 400 °C, while those at 3420 and 3320 cm^{-1} closely matched the band positions for OH stretching bands in bayerite and boehmite. The band at 3580 cm^{-1} is characteristic of hydrogen bonding between adjacent surface hydroxyls (SiOH, AlOH, SiOHAl) or between surface hydroxyls and water.

The spectra for adsorbed pyridine identified the presence of HPYR, BPYR, and LPYR on the acid-activated metakaolin surface. Pretreating the acid-activated metakaolin at 200 °C prior to exposure to pyridine resulted in a decrease in the amount of Brönsted-bound pyridine and an increase in the number of thermally stable Lewis acid sites. Pretreating the acid-activated metakaolin at 400 °C reduced the thermal stability of HPYR and reduced the intensity of the LPYR band, which was tentatively attributed to the loss of surface area at this elevated pretreatment temperature.

Acid activation of alumina-containing solids proceeds via the partial dissolution of the alumina domains, while the silica tetrahedra, because of their insolubility in this medium, are transformed into an amorphous silica phase. Thus, these solids are usually described as a mixture of domains of amorphous silica and alumina where the composition of the mixture depends on the severity of the acid treatment. The results obtained here show that the acid-activated solids can be described as an intimate mixture of silica- and alumina-like phases. Consequently, the 4000−3000 cm^{-1} region in the spectra of these solids is considerably complex and is attributed to a combination of the vibration of OH groups bound to silicon and aluminum alone and in combination. Analysis of the spectra obtained during the thermal desorption of pyridine provided a suitable description of the Lewis and Brönsted acid sites generated by the acid-activation process. The information obtained using DRIFTS spectroscopy provides important information regarding the nature of the surface OH groups and the acidic nature of these materials, and contributes to their use as catalyst and catalyst supports.

Acknowledgment. This work was developed during a short stay of C. Belver at the Materials Research Institute of the Sheffield Hallam University, financed by the "Programa de Estancias Breves en España y en el extranjero de los becarios FPI" from the Ministerio de Ciencia y Tecnología, Madrid, Spain. C.B. and M.A.V. acknowledge the financial support from the Ministerio de Ciencia y Tecnología, Madrid (Research Grant ref. MAT2002-03526). C.B. acknowledges the predoctoral Grant from the Ministerio de Ciencia y Tecnología (MCyT), Formación de Personal Investigador (PFI) Program (ref. PN99-05424782).

LA048323M

(42) Ward, J. W. *J. Catal*. **1967**, *9,* 225.